Electronic Supplementary Information

Polymeric Nanorods with Aggregation-Induced Emission Characteristics for Enhanced Cancer Targeting and Imaging

Guangxue Feng,[a†] *Duo Mao,*[a†] *Jie Liu,*[a] *Chi Ching Goh,*[b] *Lai Guan Ng,*[b] *Deling Kong,*[c] *Ben Zhong Tang,*[d] *and Bin Liu*[a]*

[a] Department of Chemical and Biomolecular Engineering, National University of Singapore, 4 Engineering Drive 4, 117585, Singapore

Email: cheliub@nus.edu.sg

[b] Singapore Immunology Network (SIgN), Agency for Science, Technology and Research (A*STAR), Biopolis, 138648, Singapore

[c] State Key Laboratory of Medicinal Chemical Biology, Key Laboratory of Bioactive Materials. Ministry of Education and College of Life Sciences, Nankai University

[d] Department of Chemistry, The Hong Kong University of Science and Technology, Clear Water Bay, Kowloon, Hong Kong (China)

[†] These authors contributed equally to this work.

KEYWORDS: Cancer targeting, fluorescence imaging, nanodots, nanorods, aggregation-induced emission

EXPERIMENTAL SECTION

Materials: TPE, BTPEBT, TPETPAFN were synthesized according to literature. 1,2-Distearoyl-*sn*-glycero-3-phosphoethanolamine-*N*-[methoxy(polyethylene glycol)-2000] (lipid-PEG) was provided by Avanti Polar Lipid, Inc. (Alabama, USA). Hoechst 33342 and Qtracker 655 were purchased from Invitrogen (Eugene, OR, USA). Fetal bovine serum (FBS) was provided by Gibco (Lige Technologies, Switzerland). 3-(4,5-Dimethylthiazol-2-yl)-2,5-diphenyl tetrazolium bromide (MTT) was purchased from Sigma Aldrich. Tetrahydrofuran (THF) was distilled from sodium benzophenone ketyl under dry nitrogen immediately prior to use. Ultrapure grade 10 × phosphate-buffered saline (PBS) buffer with pH = 7.4 was purchased from 1st BASE Singapore. Milli-Q water was supplied by Milli-Q Plus System (Millipore Corporation, Bedford, USA). SKBR-3 breast cancer cells, MCF-7 breast cancer cells, MDA-MB-231 cancer cells, HeLa cancer cells, and NIH-3T3 normal fibroblast cells were provided by American Type Culture Collection.

Characterization: UV-vis spectra were recorded on a Shimadzu UV-1700 spectrometer. Photoluminescence (PL) spectra were recorded on an Edinburgh FS5 spectrofluorometer. Average particle size, size distribution, and the zeta potentials were measured by Zetasizer Nano ZS (Malvern Instruments Ltd, UK) at room temperature. The sample morphology was studied by transmission electron microscopy (TEM, JEM-2010F, JEOL, Japan) and field emission scanning electron microscopy (FESEM, JSM-6700F, JEOL, Japan). Bruker's X-ray powder diffractometer (D8 Advance, Cu Kα, $\lambda = 0.154$ nm) was used to get XRD patterns.

Synthesis of AIE nanoparticles with different morphologies: A THF solution (1 mL) containing AIEgens (1.0 mg), and lipid-PEG (2 mg) was poured into water (9 mL). This was followed by sonicating the mixture using a microtip probe sonicator at 12 W output (XL2000, Misonix Incorporated, NY). After evaporation of THF by stirring the suspension at room temperature overnight, the AIE nanoparticle suspension was purified by ultrafiltration (molecular weight cut-off 30,000 Da) at 3000 g for 30 min and filtered through a 0.45 μm

syringe driven filter. To fabricate AIE nanodots, an ultrasound sonication time of 2 min is applied. To fabricate AIE nanorods, an ultrasound sonication time of 120 min is applied. To study the mechanism of AIE nanorod formation, different sonication time of 2, 10, 30, 60, and 120 min is applied. To study temperature effects for nanorod formation, water solution is heated to 80 ºC and use for AIE nanoparticle fabrication with a sonication time of 2 min.

Cell culture: SKBR-3, MCF-7, MDA-MB-231, HeLa cancer cells, and NIH-3T3 normal cells were cultured in Dulbecco's Modified Eagle's Medium (DMEM) containing 10% FBS and 1% penicillin-streptomycin at 37 °C in a humidified environment containing 5% CO_2, respectively. Before experiments, the cells were pre-cultured until confluence was reached.

*Cellular imaging***:** SKBR-3, MCF-7, MDA-MB-231, HeLa cancer cells, and NIH-3T3 normal cells were cultured in the chamber (LAB-TEK, Chambered Coverglass System) at 37 ºC. After 80% confluence, the medium was removed; the adherent cells were washed twice with 1× PBS buffer. TPETPAFN nanodots or nanorods (0.01 mg/mL based on TPETPAFN concentration) dispersed in cell culture medium were then added to these wells. After 2 h incubation, the cells were washed twice with 1× PBS buffer. The cells were then incubated with Hoechst 33342 (5 μg/mL) for 20 min. After twice washing with 1× PBS buffer, the cells were imaged by Nikon A1 confocal laser scanning microscopy (CLSM).

Endocytosis study. SKBR-3 and HeLa cancer cells were cultured in (LAB-TEK, Chambered Coverglass System) at 37 ºC. After 80% confluence, the medium was removed; the adherent cells were washed twice with 1× PBS buffer. Selected cells were pretreated with different endocytosis inhibitor: cytochalasin D (5 μg/mL), LY294002 (20 μg/mL), Chlorpromazine (5 μg/mL), nocodazole (5 μg/mL), methyl-*β*-cyclodextrin (M*βCD*) (5 mM), or genistein (5 μg/mL) for 30 min before incubation with TPETPAFN nanodots and nanorods (0.01 mg/mL based on TPETPAFN concentration). After 2 h incubation, the cells were washed twice with 1× PBS buffer. The cells were then incubated with Hoechst 33342 (5

μg/mL) for 20 min. After twice washing with 1× PBS buffer, the cells were imaged by Nikon A1 confocal laser scanning microscopy (CLSM).

Cytotoxicity studies: The metabolic activities of SKBR-3, MCF-7, MDA-MB-231, HeLa cancer cells, and NIH-3T3 normal cells were evaluated using methylthiazolyldiphenyltetrazolium bromide (MTT) assay. The cells were seeded in 96-well plates (Costar, IL, USA) at an intensity of 5×10^3 cells/well, respectively. After 24 h incubation, the old medium was replaced by TPETPAFN nanorods in DMEM suspension at various concentrations. After 24 h incubation, the cells were washed with 1× PBS buffer and 100 μL of freshly prepared MTT (0.5 mg/mL) solution was added to each well. The MTT medium solution was carefully removed after 3 h incubation in the incubator. Filtered DMSO (100 μL) was then added to each well and the plate was gently shaken for 10 min at room temperature to dissolve all the precipitates formed. The absorbance of MTT at 570 nm was monitored by the microplate reader (Genios Tecan). Cell viability was expressed by the ratio of the absorbance of the cells incubated with AIE nanodots or nanorods to that of the cells incubated with culture medium only.

Animals and tumor xenograft models: All animal studies were performed under the guidelines set by the Tianjin Committee of Use and Care of Laboratory Animals, and the overall project protocols were approved by the Animal Ethics Committee of Nankai University. Male BALB/c nude mice (8-12 weeks old) were purchased from Laboratory Animal Center of the Academy of Military Medical Sciences (Beijing, China). To establish tumor-bearing mouse model, SKBR-3 cancer cells (5×10^6) suspended in 50 μL of RPMI-1640 medium were subcutaneously injected into the right axillary space of each mouse. When the tumor volume reached about 100–150 mm^3, the mice were used for the following experiments.

In vivo fluorescence imaging: SKBR-3 tumor-bearing mice were intravenously injected with 150 μL of AIE nanodots or nanorods (based on TPETPAFN concentration of 0.5

mg/mL), respectively. The mice were then anesthetized and placed on an animal plate heated to 37 ºC. The time-dependent biodistribution of TPETPAFN nanodots and nanorods in SKBR-3 tumor-bearing mice was imaged using a Maestro EX *in vivo* fluorescence imaging system (CRi, Inc.). The light with a central wavelength at 523 nm was selected as the excitation source. *In vivo* spectral imaging from 560 nm to 900 nm (10 nm step) was carried out with an exposure time of 150 ms for each image frame. The auto-fluorescence was removed using the spectral unmixing software. After the tumor-bearing mouse was sacrificed, and the liver, spleen, kidney, heart, lung, stomach, intestine, and tumor were harvested for isolated organ imaging with Maestri system (Cri, Inc.). The tumor was further cut into sections (6 μm) with a microtomy at 24°C (Leica CM Rapid Sectioning Cryostat) and imaged by CLSM.

Evaluation of in vivo toxicity: Healthy BALB/c mice were randomly assigned to 3 groups and each group contained 4 mice. On day 0, the mice in one group were intravenously injected with 150 μL of TPETPAFN nanodots or nanorods (based on TPETPAFN concentration of 0.5 mg/mL) or without any treatment. After the injection, 9-day follow-up experiments were conducted, in which the weights of all the mice were scrutinized. On day 9, the mice were sacrificed and the blood was collected through cardiac puncture at the time of sacrifice for blood chemistry analyses by Tianjin First Central Hospital. Hematoxylin and Eosin (H&E) staining were employed to stain the liver, spleen and kidney slices.

Statistical Analysis: Quantitative data were expressed as the mean ± standard deviation (SD). Statistical comparisons were made by ANOVA analysis and Student's *t*-test. P value < 0.05 was considered statistically significant.

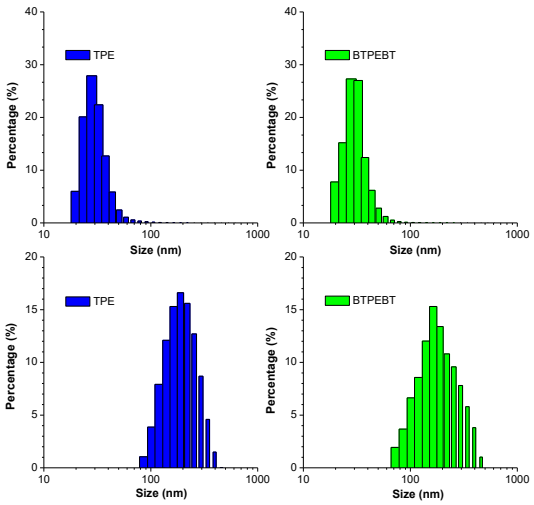

Figure S1. Hydrodynamic size distributions of AIE nanodots (top) and nanorods (bottom).

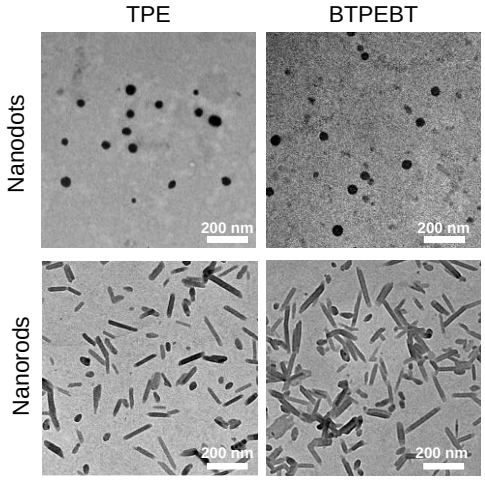

Figure S2. TEM images of TPE and BTPEBT based AIE nanodots and nanorods.

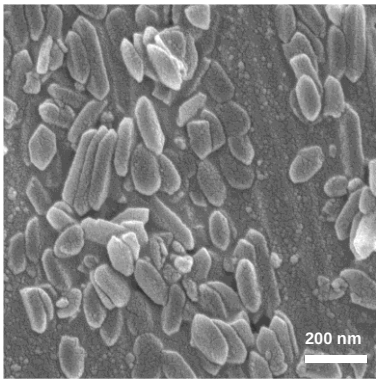

Figure S3. SEM image of TPETPAFN nanorods.

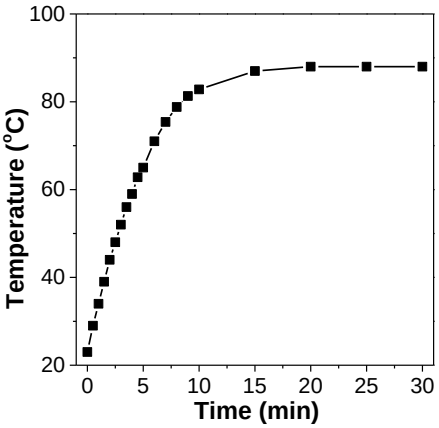

Figure S4. Temperature changes of the THF/Water mixture upon ultrasound sonication.

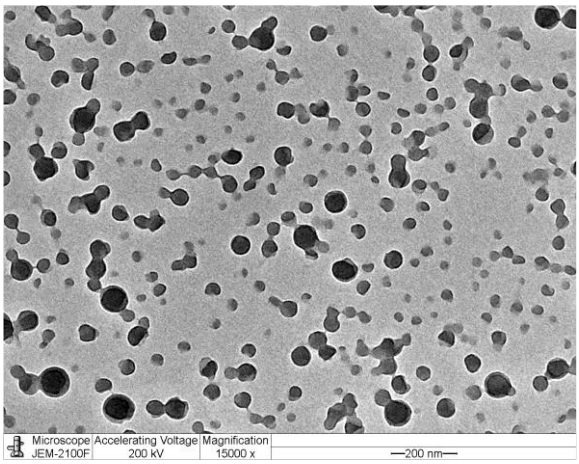

Figure S5. TEM image of TPETPAFN nanodots fabricated at 80 °C with 2 min sonication.

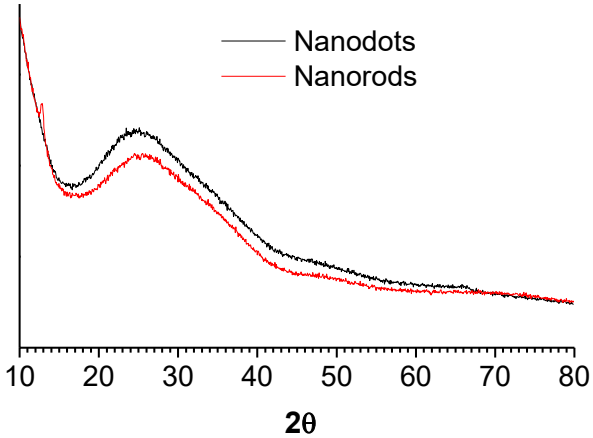

Figure S6. XRD spectra of TPETPAFN nanorods and nanodots.

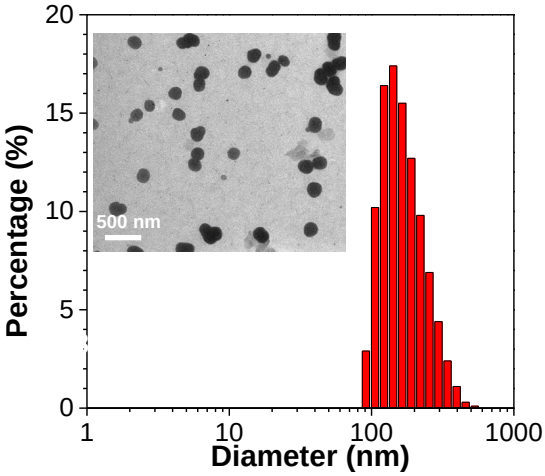

Figure S7. Size distribution and TEM image of TPETPAFN nanodots with size around 180 nm.

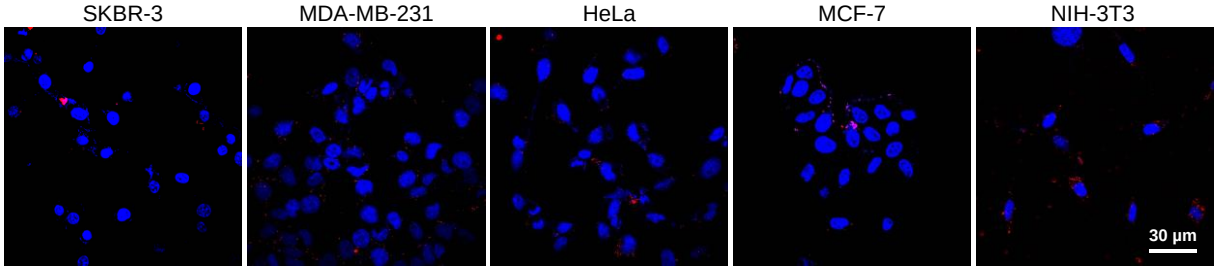

Figure S8. Confocal images of different cell lines after 2 h incubation with TPETPAFN nanodots with size around 180 nm (0.01 mg/mL based on TPETPAFN concentration)

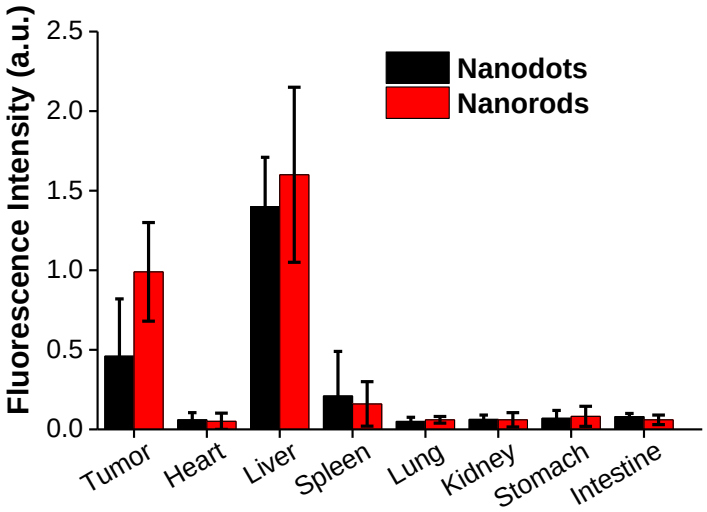

Figure S9. Average fluorescence intensities detected from organs extracted from mice treated with TPETPAFN nanodots or nanorods.

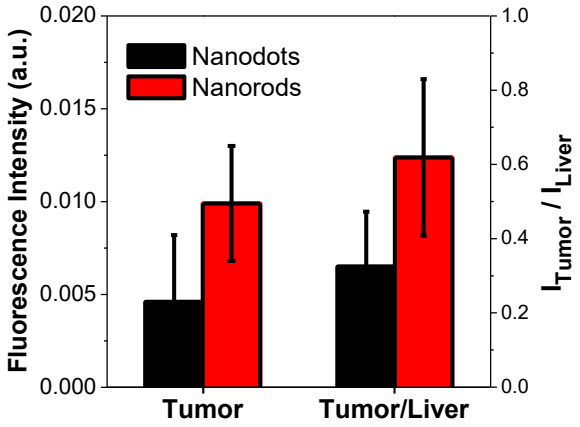

Figure S10. Tumor fluorescence intensities and the tumor/liver fluorescence intensity ratios for TPETPAFN nanorods and nanodots.

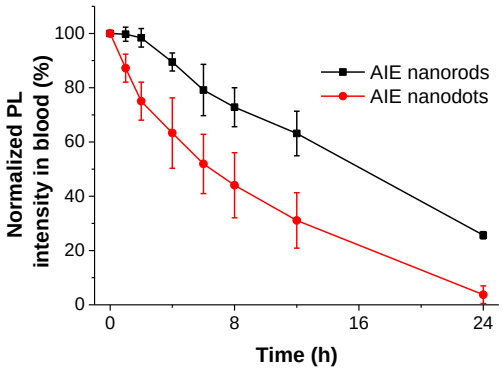

Figure S11. Plot of fluorescence changes of AIE nanodots and nanorods in blood as a function of post-injection time.

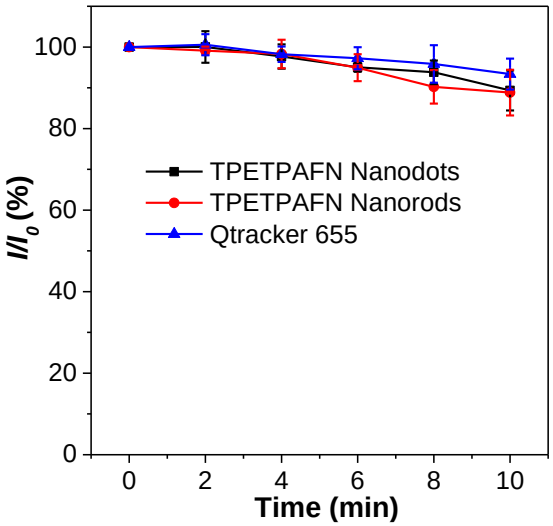

Figure S12. Fluorescence intensity changes of TPETPAFN nanodots, nanorods, and Qtracker 655 after 10 min continuous laser scanning (100% power of WLL laser equipped on Leica SP8 confocal microscope at wavelength of 510 nm).

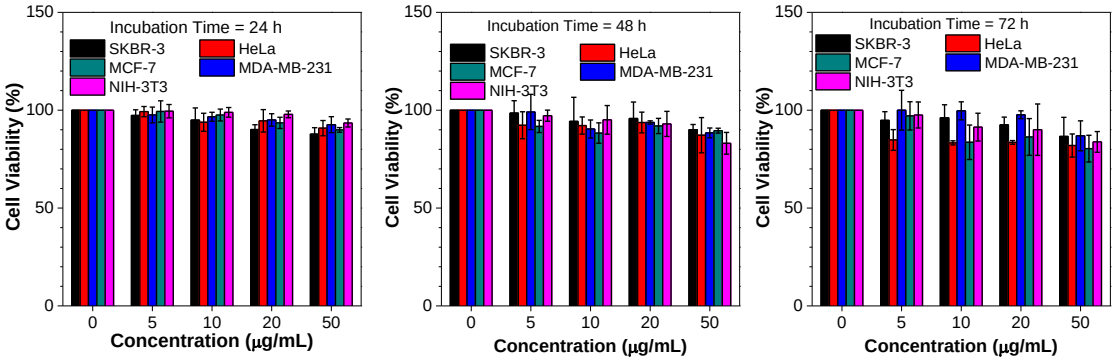

Figure S13. Viabilities of different cells after 24, 48 or 72 h incubation with TPETPAFN nanorods at varied concentrations.

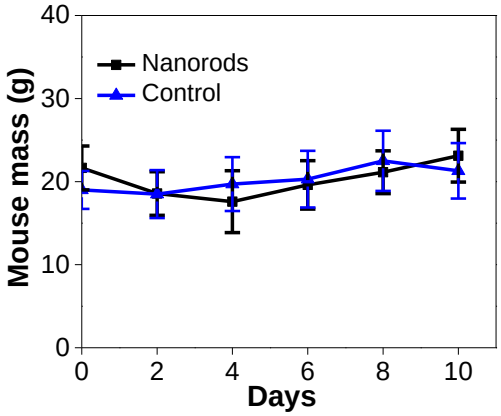

Figure S14. Mouse weight changes over 10 days after intravenous injection of TPETPAFN nanorods (150 μL/mouse, 0.5 mg/mL based on TPETPAFN concentration).

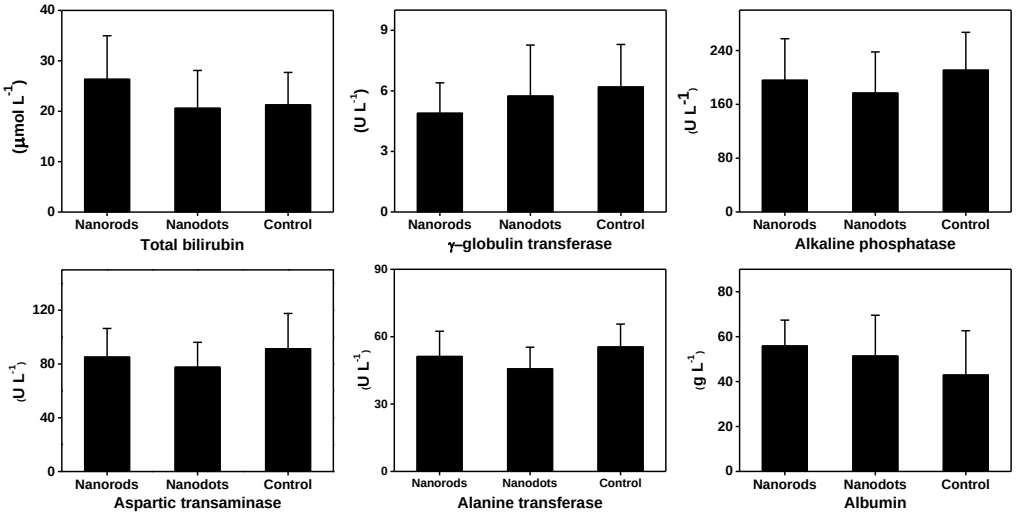

Figure S15. Blood chemistry tests of mouse after intravenous injection of TPETPAFN nanorods or nanodots (150 μL/mouse, 0.5 mg/mL based on TPETPAFN concentration).

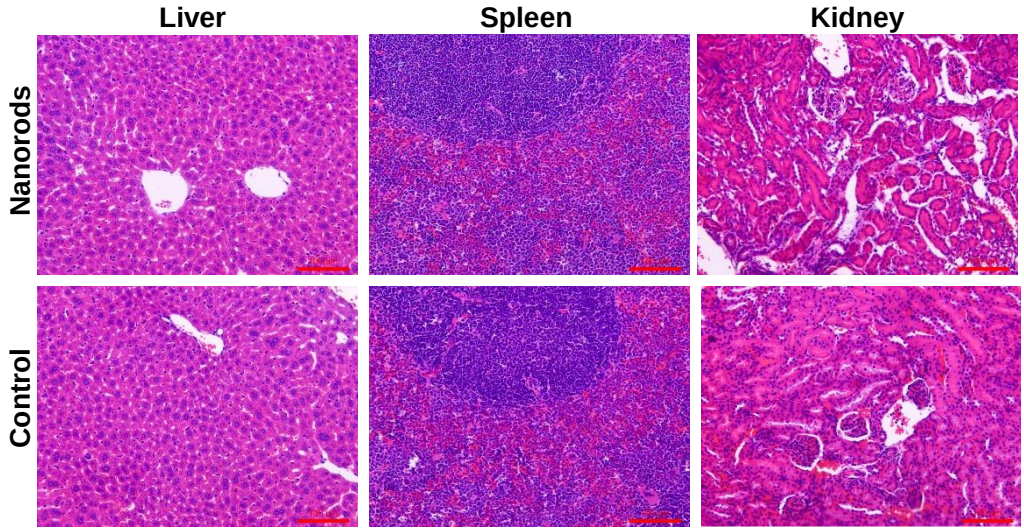

Figure S16. H&E stained liver, spleen, and kidney from mouse treated with TPETPAFN nanorods and without any treatment (Control).